World Conference on
Timber Engineering
Oslo 2023

A NEW METHOD FOR MODELLING TEMPERATURE WITHIN STEEL BAR - TIMBER COMPOSITE BEAM USING DATA BY BURNING TEST

Shizuka Matsushita[1], Shinichi Shioya[2]

ABSTRACT: In light of the current climate crisis, there has been much recent interest in using timber structural members in large buildings, since timber is as renewable natural resource, and moreover, in severe earthquake prone zones, such as Japan, they are more desired on the grounds of light weight of timber members. We are developing a frame system formed by hybrid timber members reinforced with deformed steel bars (i.e. rebars) using epoxy resin adhesive. In order to practice the system, it is necessary to investigate fire resistance performance of the members. We conducted a 60-minute burning test of one specimen of the composite beam. The results will be reported in this WCTE2023[1]. This paper proposes a method for modelling temperature within beam specimen by using finite data obtained by the burning test.

KEYWORDS: Fire, Burning margin, Hybrid timber, Deformed steel bar, Beam

1 INTRODUCTION [345]

S.Shioya, (author [2]), has proposed a structural system for building construction, adopting Hybrid Glulam Timber members using Steel bars (HGTSB, nicknamed “Samurai” in Japan) [2]. Three-buildings were built with the system. One of them adapted two HGTSB beams, for a trial, at 11th floor of high-rise building, with a refractory coating authorized as two-hour fireproof timber for HGTSB beam, constructed in Tokyo, Japan, in February 2020.

On the other hand, semi-fireproof design method using burning marginal layer (charring layer) for HGTSB is strongly desired for low-rise and middle-rise buildings. In Japan, HGTSB member is defined as a new kind of structural member; Japan Building Standards Law does not allow application of general semi-fireproof design method using burning marginal layer to HGTSB member; several burning tests of beam and column, which are loaded with maximum weight of long-term design, are requested. However, difficulties of practice of the burning test pose at the point of test machine capacity and selection of failure mode of beam during its burning, because bending capacity of HGTSB beam is approximately 3-4 times as much as that of conventional Glulam beam.

The key to the solution of the difficulties is to develop new method for modelling temperature distribution within beam using several finite data of temperature measured during the burning test. The position and the number of the measuring points need to be selected so as to prevent bending capacity and shearing capacity of the beam from deteriorating. Thus, the new method is need. Moreover, verification of the capacity calculated using the modelled temperature distribution and reduction ratio of strength and elasticity of wood of beam is necessary to be conducted by using capacities obtained by loading during the beam burning test.

We conducted 60-minute-burning test of a timber-steel rebar composite beam and will report its outline and experimental results in WCTE2023[1]. This paper reports results of temperature variation inside the glulam timber and a new concept of modelling of temperature within the beam with finite measured temperature data.

2 OUTLINE OF BURNNING TEST

Details of burning test will be described in Literature 2 in this WCTE2023. Please refer to it. Outline of the test is described below.

2.1 SPECIMEN

Figure 1 illustrates measured cross-sections of specimen and a resisting area in the section expected after 60-minute burning. Figure 2 (in next page) illustrates a side view of the specimen and positions of foil strain gauge and thermocouple. Figure 3 illustrates 4 cross-sections of the specimen and positions of thermocouples in each cross-section. Main cross-section of beam is section II-IV with

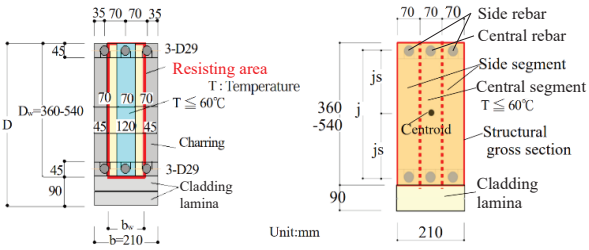

Figure 1: *Cross-section and resisting segment and area after 60 - minute burning*

[1] Shizuka Matsushita, Department of Architecture, Kagoshima University, Japan, k7422990@kadai.jp
[2] Shinichi Shioya, Department of Architecture, Kagoshima University, Japan, k7347039@kadai.jp

https://doi.org/10.52202/069179-0212

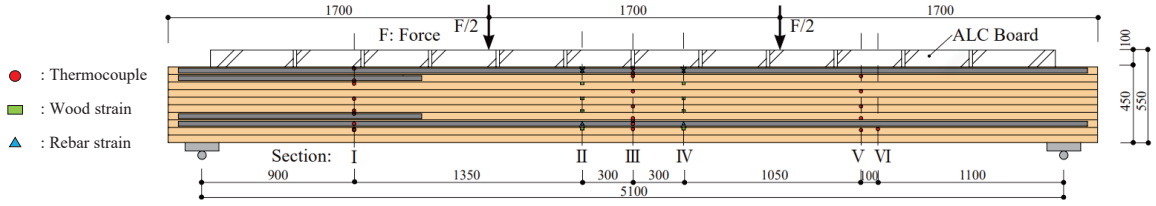

Figure 2: *Side view of specimen and positions of strain gauge and thermocouple*

one tier rebar lamina, in which 3 rebars were embedded, on upper and lower of beam cross-section. The left-hand section I was prepared to investigate effects of the amount and the number of rebars on elevated temperature of wood during burning. The lamina is Cryptomeria Japonica; lamina composition of beam is adhered to Japanese Agricultural Standard E65-F225. Rebar diameter is D29(diameter=29mm) and its grade is SD390(Nominal yielding strength: 390N/mm^2). Adhesive is typical resorcinol resin adhesive for laminating laminas.

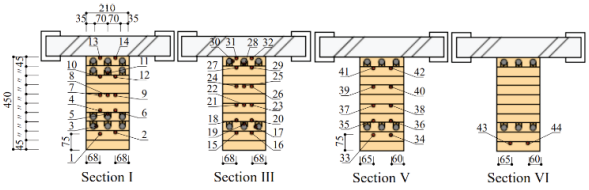

Figure 3 : *Cross-section measured in specimen and positions of thermocouple*

2.2 STRAIN AND TEMPERATURE MEASUREMENT

In Figure 2, locations of thermocouples are shown. Strain in wood and temperature of rebar were measured. Numbering of mark "No." is for thermocouple.

2.3 LOADING

Loading employed four-point bending such as the side view of specimen shown in Figure 2; magnitude of bending moment at mid-span of the specimen was selected to be value of allowable moment for long-term selected to be value under long-term loading design. Value of shearing force of both side shear spans was 10% higher than its allowable shear force for long-term loading design. Force/F.

2.4 HISTORY OF TEMPERATURE

The burning test was conducted on September 28, 2021 at 13:00 (its room temperature: 25.6°C) in a combustion furnace (ISO843-1 compliant furnace) at the Japan Testing Center for Construction Materials. During introducing initial force, deflections and strains in the elastic range were measured. Temperature during 60-minute burning test was controlled to adhere to ISO-fire exposure temperature curve. To capture capacity of the specimen by loading to fracture, a burning time of 5 minutes and 20 seconds after 60-minute burning passed was added; temperature of furnace was maintained at a constant temperature (945°C) by combustion.

3 CHANGE IN TEMPERATURE OF WOOD AND REBAR WITHIN GLULAM TIMBER DURING BURNING

Figure 4, Figure 5, and Figure 6 in the next page show the temperature variation of each measuring point. Figure 6(g) shows the variations of all measuring points for each section; Figure 4 shows that of section I and Figure 5 shows that of section III. The number on curves refers to the number of the measuring point in Figure 6(g); RC refers to the center rebar; RS dose to the side rebar; Va dose to a measured point at which temperature was presumed to increase due to water vapor generated by burning of wood.

Cal.1, Cal.2, and Cal.3 are curves based on an estimation method proposed in Chapter 4. Timber is a natural material, and thicknesses and densities of spring woods and autumn wood are not the same. Timber is not a uniform material to begin with. As the temperatures were measured at one point, it is necessary to analyse trend of temperature variation based on the assumption that the conditions of the material around the measuring point will be slightly different even at same depth from surface of timber, and that there will be some variation in the measured data.

3.1 UPPER LAMINA ENBEDDED WITH REBAR

Figure 4 (b) and Figure 5(b) show temperature variation of the upper lamina.

31V$_a$ and 32V$_a$ in Figure 5(b) show that the temperatures increased rapidly in 20-30 min, maintained about 90°C for 30-50 min, and increased slowly thereafter.

The cause is assumed to be that deflection at mid-span increased space between the upper surface of beam and the ALC board over beam, allowing hot air and flame to penetrate, causing the temperature there to rise quickly and water vapor from the burning of the timber to be suspended. Although RC28V$_a$ was in the same lamina, the temperature rise was extremely slow, but according to Figure 5(f), the rate of rise was faster than that of RC19, i.e., the central rebar at the lower. That time was almost the same as the time when 31Va and 32Va rose rapidly and reached about 90°C.

https://doi.org/10.52202/069179-0212

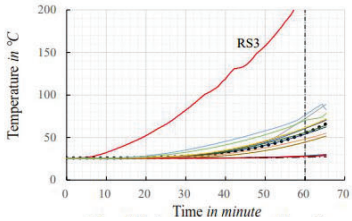

Figure 4(a): *Whole in section I*

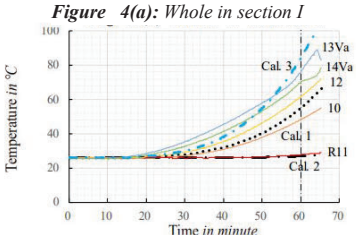

Figure 4(b): *Upper in section I*

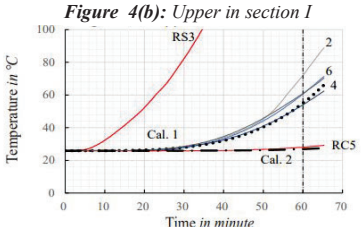

Figure 4(c): *Lower in section I*

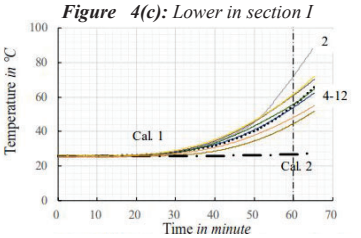

Figure 4(d): *Side line of wood in section I*

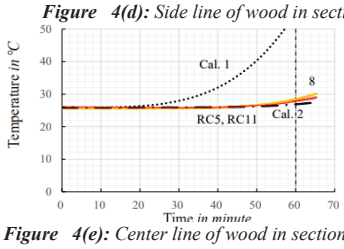

Figure 4(e): *Center line of wood in section I*

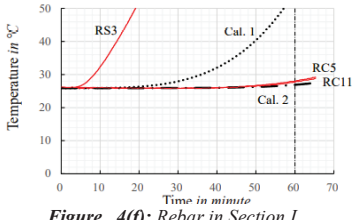

Figure 4(f): *Rebar in Section I*

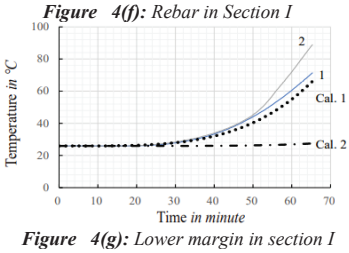

Figure 4(g): *Lower margin in section I*

Figure 4: *Variations of temperatures in section I*

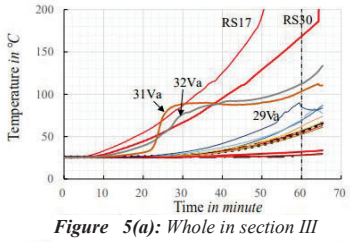

Figure 5(a): *Whole in section III*

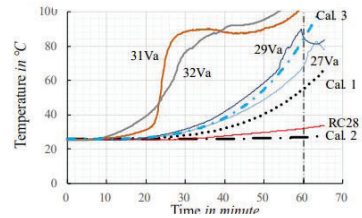

Figure 5(b): *Upper in section III*

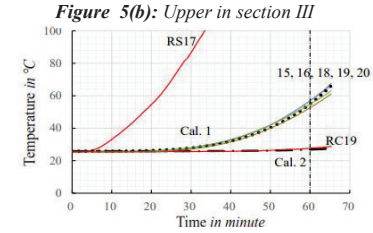

Figure 5(c): *Lower in section III*

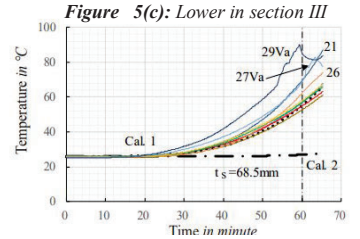

Figure 5(d): *Side line of wood in section III*

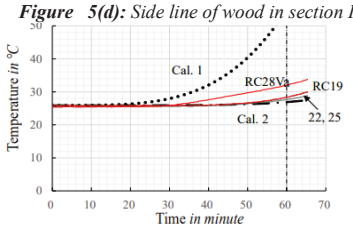

Figure 5(e): *Center line of wood in section III*

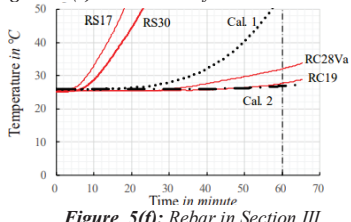

Figure 5(f): *Rebar in Section III*

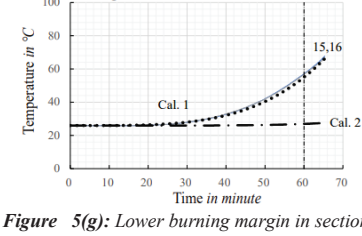

Figure 5(g): *Lower burning margin in section III*

Figure 5: *Variation of temperatures in section III*

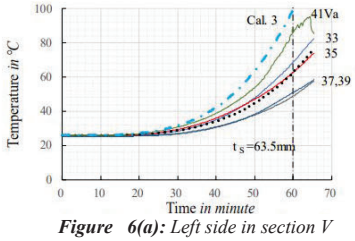

Figure 6(a): *Left side in section V*

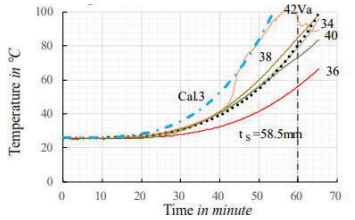

Figure 6(b): *Right side in section V*

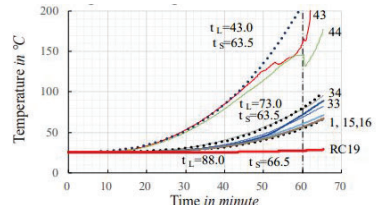

Figure 6(c): *Lower burning in section I, III, V, and VI*

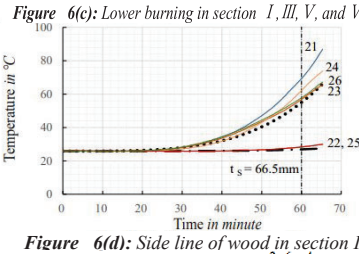

Figure 6(d): *Side line of wood in section III*

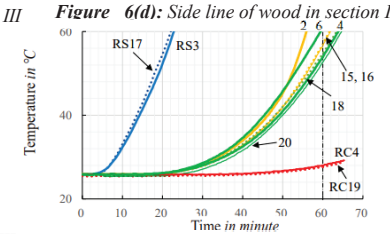

Figure 6(e): *Lower in section V*

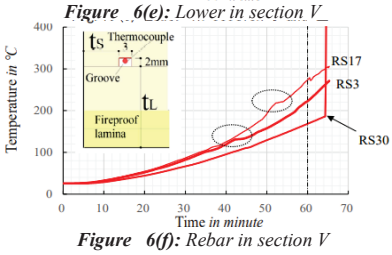

Figure 6(f): *Rebar in section V*

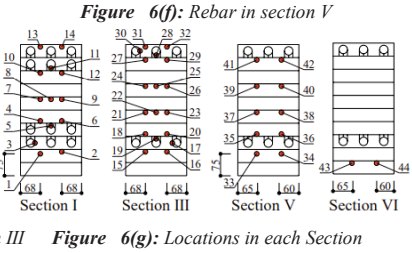

Figure 6(g): *Locations in each Section*

Figure 6: *Variations of temperatures in Section in V, etc.*

https://doi.org/10.52202/069179-0212

A similar trend was observed for $13V_a$ and $14V_a$ in Figure 4(b), but it is less pronounced than for $31V_a$ and $32V_a$ in Figure 5(b). The reason may be that section I had a resulting in a slower rate of temperature increase. $27V_a$ and $29V_a$ in Figure 5(d), 41Va in Figure 6(a), and $42V_a$ in Figure 6(b) are also considered to be affected by the same effect.

3.2 LOWER REBAR LAMINA

Figure 4(c) and Figure 5(c) show temperature variation of the lower rebar lamina. Temperatures of the side rebars/RS3 and RS17 increased rapidly after 6 minutes. In Figure 4(g), temperature of 2 at section I was 72°C at 60 minutes. In Figure 6(e), temperatures of wood (4,6,15,16,18,20) at border of lower rebar lamina of the central segment of except for the 2 were below 60°C. This demonstrates that the lower border of the central column segment in Figure 1(b) is almost suppressed below 60°C.

3.3 WEB

The points have a horizontal depth/t_s (see Figure 6(f)) of 68.5 mm. t_s is horizontal depth from the side surface of beam to the width of the groove (3 mm) where the thermocouple is placed. Figure 6(a) shows the temperature variation at the border with t_s of 63.5 mm in cross-section V and Figure 6(b) shows the temperature variation at the border with t_s of 58.5 mm in the same cross-section. As t_s decreased, temperature increased in 60 minutes, and except for 36 at 58.5 mm in Fig. 6(b), the temperatures were above 70°C. Figure 5(d) shows temperature variation from 21 to 26 in cross- section III. In contrast to the temperatures at t_s of 68.5 mm (21, 23, 24, 26), temperature at center of the width (22, 25) in Figure 5(e) hardly increases at all. Even if there is some difference in the temperature variation at the border of the central segment width 70 mm, temperature near the center of the width decreases rapidly, and effect of the variation on the center rebar is considered to be small.

From the above discussion, it can be judged acceptable to calculate the capacity of the center segment as less than 60°C, except for upper surface of the rebar lamina at top of beam as mentioned in Section 3.1.

3.4 EFFECT OF THICKNESS OF CLADDING LAMINAS TO THE LOWER PORTION

Figure 6(c) shows temperature variation of the cladding lamina. The vertical depth /t_L (Figure 6(f)) of 43 and 44 in cross-section VI from the lower surface was 43.0 mm, thus reaching 150°C in 60 min; t_L of 33 and 34 in cross-section V was 73.0 mm, thus 69 ° C and 79°C, respectively; t_L of 15 and 16 in section III was 88.0 mm, thus both were 57°C. The t_L of 15 and 16 in cross-section III was 88.0 mm, so they were both suppressed to 57°C. RC19, the central rebar near the lower of cross-section III, was 27.6°C, hardly increasing from the initial 25.6°C. The center of the rebar in RC19 was almost 105 mm deep from both the lower surface and side surface of beam, and it can be concluded that that depth suppressed the temperature increase.

Figure 6(d) shows temperature variation of 21-26 of web of the cross-section III. 21, 23, 24, and 26 at the boundaries of the central segment were 56-68°C in 60-minute, while 22 and 25 in the middle of the beam width were both 28 ° C, hardly any increase in temperature. Considering this, the same depth from the lower at the width-middle position may be also quite low, close to 28°C, because 33 and 34 in cross-section V were 69°C and 79°C, respectively as mentioned above. These results suggest that even with a thickness of 75 mm of cladding laminas, the increase in temperature of the central rebar at the bottom of beam is suppressed in a 60-minute burn. However, from the viewpoint of providing extra strength for 60-minute burning, it is desirable to keep the depth from the lower surface to the central rebar close to 105 mm, which is the same depth from the side surfaces.

3.5 EFFECT OF HEAT CAPACITY OF TWO-TIER REBAR

Because the large heat capacity of the two-tier rebar in cross-section I, 10 and 12 in Figure 4(b) were less affected by water vapor than $31V_a$, $32V_a$ in cross-section III in Figure 5(b), and the temperature of 10 and 12 is considered to have remained below 60°C after 60 minutes. On the other hand, the rebar lamina at the lower is not affected by water vapor, and Figure 6(e) shows the temperature variation of the lower lamina, comparing the two-tier/RS3 and one-tier rebar/RS17. The data for the two-tier rebar are shown as blue thick solid lines, while the data for the one-tier rebar are shown as blue dotted lines. The positions close to each other in both cross-sections are shown in the same colour. In some cases, the temperature increase is slightly slower in the cross-section of the two-tier rebar. In the side rebar shown in Figure 6(f), RS3 of the two-tier rebars rose more slowly than RS17 of the one-tier rebars, but the effect of the two-tier rebar in suppressing the temperature was not very promising.

4 CONCEPT FOR MODELLING TEMPERATURE WITHIN BEAM

The portion of wood contributing to bending capacity and shearing capacity of beam is uncharred portion. In this study, the scope limits the uncharred portion and the aim is to formulate the amount of variation in wood temperature/T from room temperature/T_r before the burning test to wood char temperature/T_c, using data of temperature measured during the burning on test.

https://doi.org/10.52202/069179-0212

4.1 FORMULATION OF TEMPERATURE-RELATIVE DISTANCE CURVE FROM CHARRING-BORDER TO A MEASURING POINT

As shown in Figure 7(a), we assume that charring border is proceeding at a constant charring rate/v_c and that measuring point/m is in the direction of the border progressing. In reality, the charring border approaches the point/m, but from the perspective of the charring border, the point/m can be considered to be approaching with a relative velocity/v_c toward. The distance/S between the point/m and the charring border is expressed by Equation (1).

$$S=d_m-v_c\cdot t \tag{1}$$

where d_m is distance between surface of beam and the measuring point/*m in mm*; v_c is charring rate *in mm/minute*; t is time of fire exposure *in minute*.

Figure 7(b) illustrates schematically relationship between temperature/T and distance/S at the measuring point/m after burning time/t passing. The distance/S decreases with the time/t, and the distance/S and the temperature/T can be plotted, yielding a T-S curve. Temperature/T of wood at the start of burning is assumed to be room temperature/T_r, which increases with the progress of charring and reaches charring temperature/T_c. The distance/S is equal to distance/d_m, at the start of burning and to zero, at reaching the charring temperature/T_c.
These two points are designated as x= d_m, y= T_r and x=0, y= T_c in Figure 7(b). These points are to be boundary points at both ends of the T-S curve, which rises linearly with decreasing S for the measuring point closer to the charring border, and rises more slowly at the beginning of burning and rises more rapidly as the charring border approaches for the more apart points.
The T-S curve can be approximated by normalizing the distance/$v_c\cdot t$ of charring progression by the distance d_m of each measuring point and by normalizing the temperature increase/ (T- T_r) by (T_c - T_r); normalizing the coordinate axes as shown in Figure 8. As results, the T-S curve is represented by Equation (2). Substituting x and y in Equation (3) into Equation (2), T is represented by Equation (4).

$$y=x^n \tag{2}$$

$$\text{where, } x=(v_c\cdot t/d_m),\quad y=(T-T_r)/(T_c-T_r) \tag{3}$$

$$T=T_r+(T_c-T_r)\cdot(v_c\cdot t/d_m)^n \tag{4}$$

4.2 EXPONENT/*n* BASED ON HARADA'S DATA

Harada et al. [3] reported a 45-minute loaded burning test on Abies sachalinensis Glulam timber beam to investigate the fire resistance performance of them, and measured temperature of the beam in detail. The model proposed above is applied to the temperature-time curves measured on the beam specimen PRF-b in the literature [3].
Specimen/PRF-b was glued with the same phenol-resorcinol resin adhesive. Figure 10(a) in the next page shows the temperature-time curve measured on PRF-b. The beam cross section and temperature measuring points

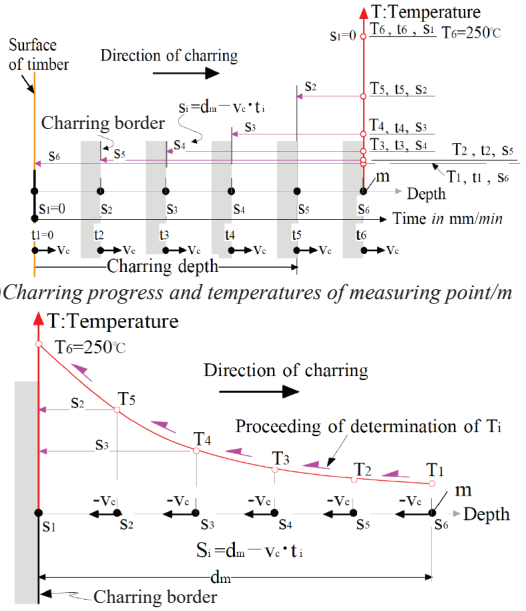

(a)Charring progress and temperatures of measuring point/m

(b)T-S curve of measuring point 'm'

***Figure 7:** A new concept for estimation of temperature distribution in uncharred region of wood in timber*

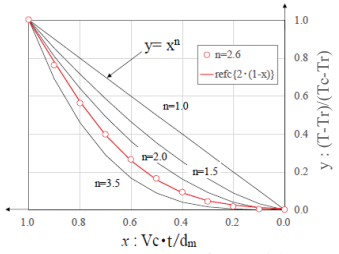

***Figure 8:** Curves by Eq.(2)*

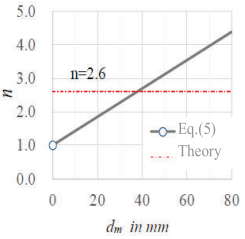

***Figure 9:** Changing by Eq.(5)*

are shown in the upper left corner of Figure 10(a). The dotted line in the Figure represents experimentally measured temperature curve.
The T-S curve drawn using S by Equation (1) is shown by coloured thin solid line in Figure 10 (a)and(b). The exponent/n was determined so that the calculated value of temperature in Equation (4) conforms to the experimental curve. The charring temperature/T_c was assumed to be 300℃ and the charring rate/v_c was set at 0.65 mm/min. The results are shown as ○ in Figure 10(c).

The y-axis is the exponent/n, and the horizontal axis is the depth/d_m. The exponent/n approaches 1.0 at zero for d_m and tends to change linearly with increasing d_m. Approximating the change with Equation (5), the coefficient/k was 0.0323.

$$n=1.0+k\cdot d_m \tag{5}$$

where k is assumed to be 0.0425 in 1/ mm

As dimensions of beam cross-section increase, exponent/n may differ from the straight line in Equation (5). It is expected to converge to a coefficient based on

https://doi.org/10.52202/069179-0212

temperature distribution during combustion of semi-infinite solid.
However, as the burning test for performance evaluation constrains cross-section dimension to be safe for burning and focus on the measured temperature data, it is out of the scope of this study to identify the convergence value.
In this study, it is enough if the exponent/n can be estimated in a form that allows the change in temperature measured in the burning test to be estimated. The T-S curve calculated with the coefficient/k in Equation (5) as 0.0323 as described above is shown in Figure 10(b) as a thin solid curve. The temperature/T - time/t curve is also shown in Figure 10(a) as a thin solid curve. The curves are coloured by the same colour for each measuring point. The rate of increase of the dotted curve was slower than the rate of the calculated curve at the temperature of 100℃, because moisture in wood becomes water vapour. In the temperature range above 120-140 °C and up to a charring temperature of 300 °C, the temperature of the calculated curves is on the safe side in terms of evaluating beam's resistance during burning, although in some ranges they are estimated to be higher than the experimental temperatures. The correspondence between measured and calculated T-S curves in Figure 10(b) is similar to that in Figure 10(a). The same study also reported the measured data of the test specimen PRF-a, which was glued together using the same adhesive with a lamina thickness of 22 mm in the cross-section in Figure 10(a), and the calculated curve for that was also confirmed to be a similar correspondence with the measured curve.
Although the coefficient/k is likely to depend on dimensions of specimen and its wood species, it can be concluded that the proposed method can be applied to historical data of temperature of burning test to model its temperature variation.

4.3 EXPONENT "*n*" BASED ON THE TEST

Figure 11 shows T-S curves based on data from each measuring point in this test. It is shown up to the end of the burning test; Figure 11(e1) shows the T-S curve for rebars. In this study, amount of loading was selected for the cross-section of the one-tier rebar at the middle of the span, so the exponent/n in Equation (4) was determined to fit the temperature data for cross-sections III, V and VI. The result adopted 0.0425 (1/mm) of n.

The charring temperature/T_c was assumed to be 250°C, T_r was assumed to be 25.6°C, the internal temperature before the burning test, and the charring rate v_c was assumed to be 0.65 mm/min with reference to Eurocode 5.
On the basis of the above approach, various constants were specified.
Figure 8 in the previous page shows the curves for varying n in Equation (2). Symbol '○' indicates the calculated value when n was assumed to be constant value of 2.6. Red curve in Figure 8 is the curve of the complementary error function (y=erfc(2-(1-x)) of the equation for the theoretical solution of temperature inside the semi-infinite solid during burning.
The ○ and red curves are almost identical, which means that Equation (2) can also approximate the curve of the equation of its theoretical solution, within the range of application. Figure 9 shows the variation of the exponent n according to Equation (5) with k of 0.0425. When d_m is close to zero, the shape of the T-S curve becomes steeper as surface of timber charrs at the initial burning, so approximating temperature with a straight line is not a major problem.

4.4 TEMPERATURE VARIATION AND COEFFICIENT/ *k*

Value of the coefficient k in Equation (5) was selected to minimize the standard error between the temperature measured at each position and the value calculated using Equation (4) for Figure 11 (b1), (c1), (c2) and (d1) of the cross section of the one-tier rebar during 60-minute burning.
In this case, the value that minimizes the standard error for the data of cross-section III where the temperature closest to the border of the central segment in Figure 1(b) was measured, was found to be 0.0425.
The d_m of each measuring point in wood was assumed to be the smaller distance between the horizontal depth/t_s and the vertical depth/t_L shown in Figure 11(a1), taking into account dimensions of the thermocouple groove.
Table 1 in the next page lists measured temperatures, their standard deviation/SD, calculated values, and their standard error/SE of the calculated values relative to the measured values for Figure 11 (b1), (c1), and (c2), where t_s (here equal to d_m) is the same for each position.

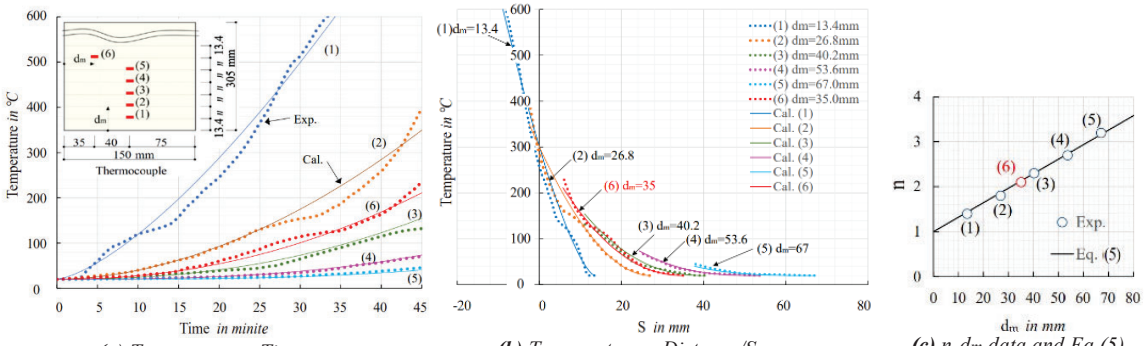

(a) *Temperature - Time curves* ***(b)*** *Temperature – Distance/S curves* ***(c)*** *n-dm data and Eq.(5)*

Figure 10: *Temperature – Time relationship of specimen/PRF-b of Harada's burning test for Japanese Abies* [3]

https://doi.org/10.52202/069179-0212

The position closest to the border of the central segment is Figure 11(b1), i.e., t_s=66.5mm, and the calculation error/SE for Equation (4) is 2.21°C. As temperature within the central segment is lower, its standard error is small.

Figure 11(d1) shows two positions (t_s=58.5, 63.5mm, t_L=75mm) of the cladding lamina in cross-section V. The measured values are almost the same change, which is almost estimated by the red calculated curve. Figure 11(d2) shows a cross-section VI with a depth t_L of 43 mm from the bottom surface, which is the position where charring will take place and where the temperature becomes high, as can be seen in Figure 12(b). Above 100°C, the temperature calculated by the curve is higher than the measured value. However, above 100°C, the reduction in the strength of wood is extremely large [4], and estimating the capacity of beam on the safe side is not a problem.

4.5 TEMPERATURE OF UPPER LAMINAS

Figure 11(a3), (b3) and (c3) show variation of temperature of upper surface of beam and wood on the underside of the rebar lamina immediately below it. Temperatures at the upper surface of beam/13V_a, 14V_a, 31V_a, 32V_a, indicate the temperature affected by water vapor, as thermocouples at the measuring points were in direct contact with the water vapor that might be stayed as mentioned above. Wood temperatures are estimated to be close to the temperature directly below the rebar lamina, i.e., 27V_a, 28V_a, 29V_a, 41V_a, 42V_a. Red one-dot curve in the Figures is curve of the calculated value according to Equation (4). The curve underestimates temperature of the wood directly below the rebar lamina (e.g., 27V_a as

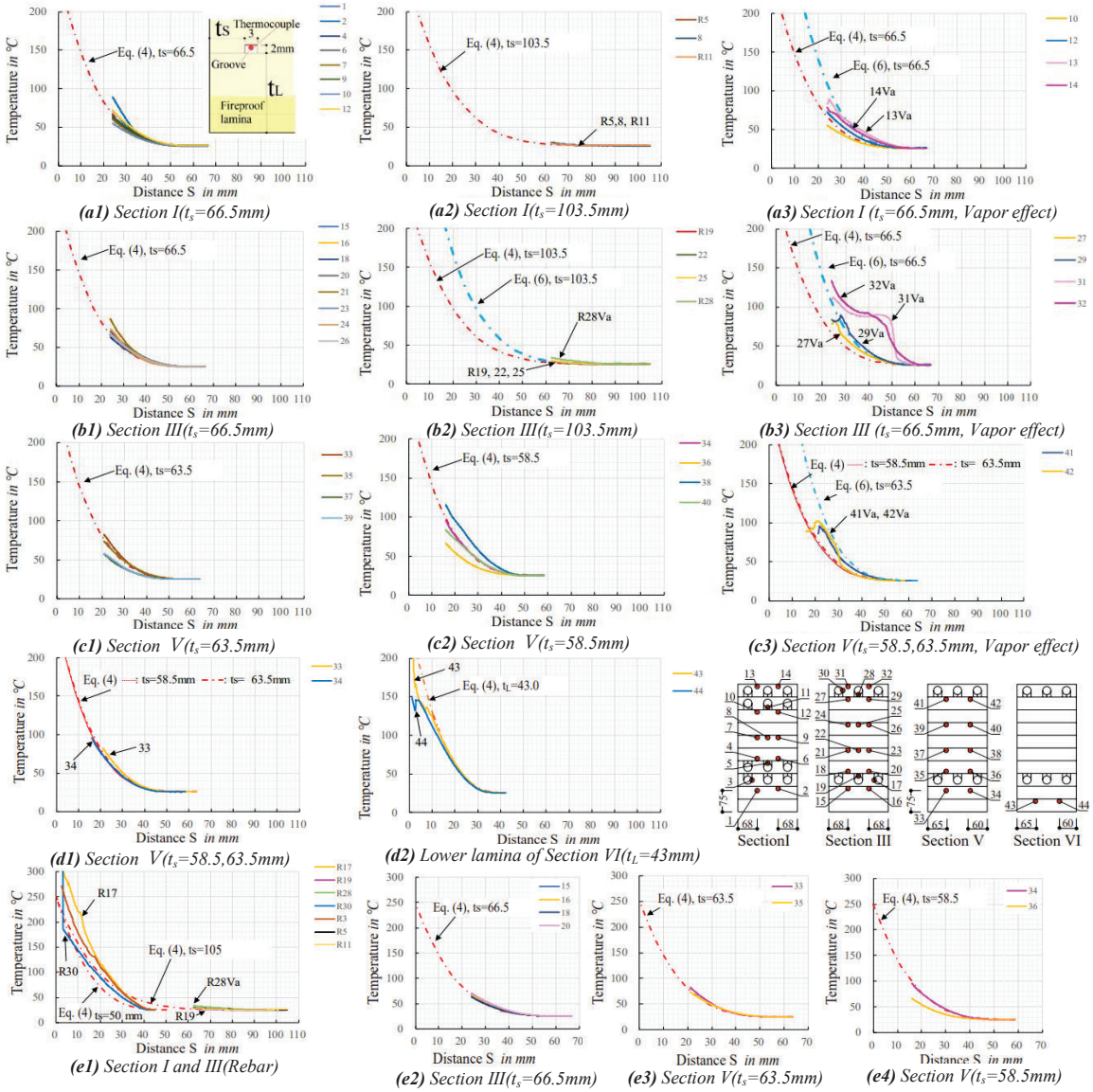

Figure 11: *Temperature/T-Distance/S relationship in wood by experiment and curves calculated by Eq.(4) and Eq.(6)*

https://doi.org/10.52202/069179-0212

described above). In this study, it was assumed to approximate the temperature variations in the upper rebar lamina with the following Equation (6), in which the temperature increase in the second term on the right side of Equation (4) is multiplied by 2.0 to obtain a relatively accurate estimate of the temperature variations.

$$T=T_r+2.0\cdot(T_c-T_r)\cdot(V_c\cdot t/d_m)^n \qquad (6)$$

Curve based on Equation (6) is shown as light blue dotted line. In Figure 11(a3), (b3), and (c3), the light blue curves roughly estimate the variation in temperature, i.e., $27V_a$, $29V_a$, $41V_a$, $42V_a$ of wood below the upper rebar lamina. In Figure 11(b3), temperatures of $31V_a$ and $32V_a$ on the upper surface of beam approach the temperature in the light blue curve after 60-minute burning. In terms of estimating the temperatures of this 60-minute burn, it is seemed that they can be estimated using Equation (6). The value of 2.0 needs to be verified by adding data from other burning tests in the future.

4.6 TEMPERATURE OF WOOD AROUND SIDE REBAR

Figure 11(e1) shows curves of rebars in cross-sections I and III. The curves by red one dot line were calculated by Equation (4), where d_m was assumed to be 50 mm (=35+15) for the side rebar as the side position near the central rebar, and d_m was assumed to be 105 mm for the central rebar as the center of the rebar. As temperature of the central rebar hardly rises, the difference of the calculated value to experimental value is almost negligible. However, temperature of the side rebar reached the charring temperature early because wood cover thickness on the side of the side rebar was 20 mm, and measured temperature of the rebar was larger than the calculated temperature because the thermal conductivity of rebar is larger than that of wood.

Figure 11(e2), (e3), and (e4) show variations of temperature of wood around the rebar lamina at the lower. Figure 13(a) and (b) show positions of thermocouples around the lower rebar lamina. Except for thermocouple 36 in Figure 11(e4), all positions follow the curve of the calculation. In Figure 12(b), wood around the side rebar was deeply charred, but as seen in Figure 11(e2), no increase up to the charring temperature was measured at the location near central side of the side rebar. However, considering charring condition in Figure 12(b), it is safe to assume that wood around the side rebar which is surrounded by pink line in Figure 13(c), cannot resist in burning for 60 minutes.

Table 1: *Depth/t_s of measurement point, distance/S and temperature after 60-minute burning, and temperature/T calculated by Eq.(4)*

Section	Fig.25	n	t_{so}	t_s	S	Temperature *in* ℃			
				in mm		Experiment		Calculation	
						Ave.	SD	Cal.	SE
III	(b1)	8	68.0	66.5	27.5	59.4	4.4	55.0	2.21
V	(c1)	4	65.0	63.5	24.5	57.8	8.2	62.8	4.81
V	(c2)	4	60.0	58.5	19.5	76.6	15.0	80.4	7.72

n: The number of data, t_{so}: Depth of wood from side surface of beam to measure point, t_s: T_{so}-3/2, SD: Standard deviation, SE: Standard error

4.7 RELATIONSHIP BETWEEN TEMPERATURE AND BURNING TIME AT EACH MEASURING POINT

Given the charring rate/v_c and the time of burning/t, the temperature at each point can be calculated using Equation (4) or Equation (6) to obtain a T-t curve of relationship between temperature and burning time. Here, the coefficient/k was assumed to be 0.0425 as mentioned above, charring temperature T_c of cedar wood was assumed to be 250°C [5], T_r was assumed to be room temperature of 25.6°C before the burning test, and the charring rate v_c was assumed to be 0.65 mm/min. d_m follows Section 4.4. The calculation results are shown as curves as Cal.1-Cal.3 in Figure 4-Figure 6. Cal.1 is the curve calculated for the measuring points close to the border of the central segment and Cal.2 is the curve calculated for the central position of beam width, i.e., the central rebar position. Cal. 3 is the curve calculated using Equation (6), which takes into account the effect of water vapor on the upper rebar lamina. The variation of calculated temperature is in good agreement with the experimental variation.

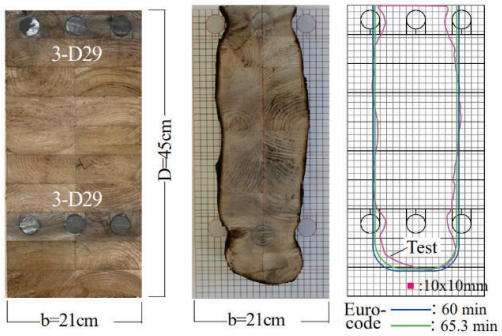

(a)For specimen *(b) Specimen after 65.3-minute burning test*

Figure 12: *A cut cross-section and an uncharred wood in the cross-section and curves calculated by Eurocord 5*

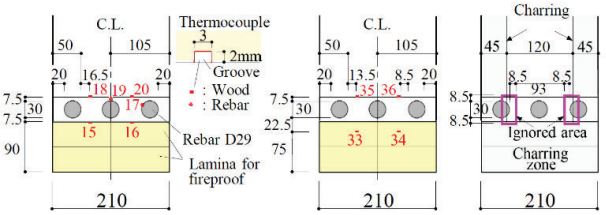

(a) Section III *(b) Section V* *(c) Invalid area*

Figure13: *Portion of thermocouples and ignored area*

https://doi.org/10.52202/069179-0212

5 TEMPERATURE DISTRIBUTION OF UNCARBONIZED CROSS-SECTION WITHIN GLULAM TIMBER DURING 60-MINUTE BURNING

The beam section is divided into charred area and uncharred area as shown in Figure 14; the shortest depth of dy, dx_1, dx_2 is assumed to be d_m, where dy is depth from the lower surface and dx_1 and dx_2 are depth both sides of the beam respectively. The charring border of the outward corner of the lower surface of the beam is circular as shown in Figure 12(b), due to the burning of the lower surface and the side faces; in Eurocord 5[4], a point O is assumed to be inside from those faces at a distance twice the charring depth/$v_c \cdot t$, as shown in Figure 14, and the arc was assumed to be as 1/4 of a circle with the charring depth/$v_c \cdot t$ as radius. Here, in the uncharred area at its outward corner, temperature/T of wood at the position of the arc of concentric circles of radius/r_o centred at point O was assumed to be isothermal and equal to temperature due to burning in one direction on the bottom or side surface. Figure 15 shows temperature distribution in the uncharred area within the cross-section of this beam calculated for a 60-minute burning. The cross-section was divided into 84 sections in the beam width direction and 180 sections in the beam height direction. In future calculations of capacity of beam, it is assumed that wood in the pink range in Figure 13(c) do not resist, and effect of the rebar on temperature of the wood area is ignored.

Figure 15(a) shows the 3-dimensional distribution of isotherms in the right half of the beam cross-section in Figure 15(b). It is shown in the view from the top surface of the beam to the bottom surface. Temperature in the charred area is shown as 250°C. The temperature decreases rapidly as its position moves toward the interior. The x-y co-ordinate axes in the cross-section are indicated in Figure 15(b). The origin of x and y is assumed to be the centre of the beam width at the border between the lower surface of the structural section and the cladding lamina. The y is positive upwards, whereas the negative range of y means the range of the cladding lamina.

Figure 15(c) shows curves of temperature along the beam height. The curves indicate the center of the beam width (x=0 mm), the 50°C border (x=±36 mm), the 60°C border (x=±40.5 mm) and the centre of the side rebar (x=±70 mm). The temperature at the center of the width (x=0mm), where the central rebar is located, is 26.9°C, almost

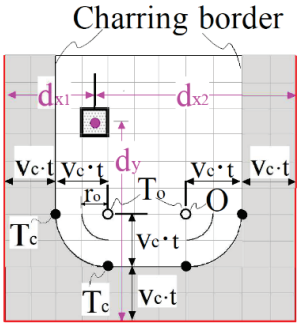

Figure14: *Distance /$dx_{1,x2,y}$ and T at the corner*

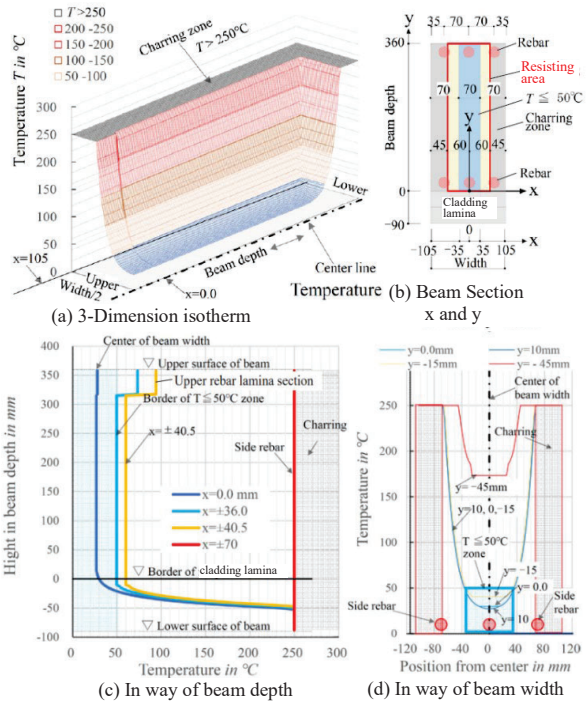

Figure 15: Temperature distribution of wood in beam cross-section after 60-minute burning calculated by the new concept

unaffected by the 60-minute burning in the structural section area ($0 \leq y$), whereas the temperature increases rapidly in the cladding lamina range ($-90 \leq y \leq 0$). This temperature distribution confirms the importance of the 90 mm thickness of cladding lamina.

Figure 15(d) shows curves of temperature in the beam width direction. The curves are for y=-15 mm in the cladding lamina, y=0 mm on the underside of the structural section area and y=10 mm in the structural section area. x=±35 mm is the width border of the central segment. Temperature in the area of the central segment within the structural section area enclosed by the blue line, i.e., $-35 \leq x \leq 35$ and $0 \leq y$, is below 50 °C, of which the area $-25 \leq x \leq 25$ is below 30 °C, resulting in the vicinity of the central rebar D29 being unaffected by burning.

From the above, it can be expected that in the case of a beam width of 210 mm, the central segment will be less than 50 °C and the temperature of the central rebar will hardly increase, even after 60-minute burning, if the thickness of the cladding lamina is 90 mm, and that the central rebar will demonstrate capacity as steel bar - timber composite beam resisting at room temperature.

https://doi.org/10.52202/069179-0212

6 SUMMARY

A method was proposed for estimating the temperature distribution inside steel bar - timber composite beam from experimental data by analysing the historical data of temperatures obtained during a 60-minute-burning test of the beam. The results are summarized as the followings:

i) A method was proposed to estimate temperature distribution in uncharred area of wood in glulam timber for any burning time within 60 minutes from the measured data of wood temperatures at limited locations in glulam timber, which reproduces the curve of the relationship between temperature at measuring point and burning time, showing temperature distribution in the cross-section during 60-minute burning.

ii) Based on the temperature distribution, beam width of 210 mm was divided into three equal sections, and the central segment of them was less than 50 °C even after 60 minutes burning, while central rebar and its vicinity were less than 30 °C (at room temperature of 25.6 °C) and were hardly affected by burning. The central segment can be expected to exhibit resistance as steel bar - timber composite beam. However, this assumes that 90-mm-thick cladding lamina are bonded to the underside of the beam.

iii) Around the side rebar, charring progresses quickly inwards in 60-minute burning, thus effect of this should be taken into account in the calculation of the capacity of beam.

iv) In 60-minute burning, the large heat capacity of the two-tier rebar in the cross-section had a small effect on the suppression of the temperature rise of wood in the glulam timber.

Note that to generalize the proposed modelling of the temperature distribution, it is necessary to generalize the method of setting the value of k for the coefficient in Equation (5).

ACKNOWLEDGEMENT

This project was funded as Grants-in-Aid for Scientific Research-B by Japan Society for the Promotion of Science.

REFERENCES

[1] S. Matsushita, S. Shioya: Burning test of steel bar - timber composite beam, Oslo, WCTE 2023

[2] S. Shioya, et al.: An innovative hybrid timber structure in Japan: performance of column and beam, Wein,WCTE 2016

[3] H. Toshiro, et al.: Temperature Dependence of Adhesive Strength and Fire Resistance of Structure Glued Laminated Timber Beams, Journal of the Japan Wood Research Society, Vol.59, No.4, pp.219-226, 2013(in Japanese)

[4] Eurocode 5, Design of timber structures - Part 1-2 General -Structural fire design, EN 1995-1-2, EUROPEAN COMMITTEE FOR STANDARD-IZATION, 2004

[5] S. Kikuchi, et al.: Internal Temperature Change of Wood by Radiation Heating, J. Hokkaido For. Prod. Res. Inst. Vol.9, No.5, 1995 (in Japanese)

https://doi.org/10.52202/069179-0212